Electronic Supplementary Material (ESI) for Journal of Materials Chemistry A.

Electronic Supplementary Information

Conductive porous organic polymer with superprotonic conductivity of a Nafion-type electrolyte

Dong Won Kang,[a] Jeong Hwa Song,[a] Kyung Jin Lee,[b] Han Guel Lee,[a] Jeong Eun Kim,[b] Hwa Young Lee,[a] Jin Young Kim,[b] and Chang Seop Hong*[a]

a. Department of Chemistry, Korea University, 136-713 Seoul, Republic of Korea.

b. Fuel Cell Research Center, Korea Institute of Science and Technology (KIST), 5, Hwarang-ro 14-gil, Seongbuk-gu, Seoul 02792, Republic of Korea

*To whom correspondence should be addressed.

Tel.: +82 232903138. E-mail: cshong@korea.ac.kr (Chang Seop Hong)

Physical Measurements. IR spectra were obtained with an ATR module using a Nicolet iS10 FT-IR spectrometer. TGA was carried out under a N_2 (99.999%) atmosphere (flow rate = 50 mL min^{-1}) in the temperature range of 25–800 °C (heating rate = 10 °C min^{-1}) using a Scinco TGA-N 1000 instrument. Powder XRD patterns were recorded using Cu Kα radiation (λ = 1.5406 Å) on a Rigaku Ultima III diffractometer with a scan speed of 2° min^{-1} and a step size of 0.02°. Deionized water used in the experiments was purified using an Aqua MAX^{TM} Basic360 series system. SEM images were acquired using a JSM-7001F scanning electron microscope. Elemental analyses for C, H, N, and S were performed at the Elemental Analysis Service Center of Sogang University. XPS data were collected at the Semiconductor & Display Green Manufacturing Research Center at Korea University using X-tool. Also, SAXS data were measured at same same center using smart lab (Target: Cu X-ray, type: Ka, wavelength: 0.154 nm, XG tube voltage: 45 kV. XG tube current: 200 mA). Solid-state ^{13}C NMR experiments were carried out using 400 MHz Avance II + Bruker solid-state NMR (spinning rate: 10 kHz, delay time (d1): 3 s, contact time: 2 ms, radio frequency: 100.4 MHz, calibration: TMS, 38.3 ppm) at KBSI Seoul Western Center. Solid-state ^{2}H NMR experiments were carried out using the same instrument (pulse program: spin echo, delay time: 5 s, probe: wide line, radio frequency: 61.42 MHz, calibration: D_2O, 4.8 ppm). EDX-SEM analysis was performed at KBSI Seoul Center using a Hitachi SU-70 instrument. Measurements to obtain solid-state T_1, T_2 values and water diffusion coefficients were carried out using a 500 MHz Avance II + Bruker solid-state NMR at the National Center for Inter-University Research Facilities (NCIRF) at Seoul National University after exposure to humid conditions for 24 h. Transmission Electron Microscopy (TEM) was carried out in Tecnai G2 20 S-Twin microscope operated.

Gas Sorption Measurements. Before sorption analysis, the samples were degassed at 120 °C under vacuum for 12 h. All gases used in the measurements were highly pure (99.999%), except for water vapor and O_2 (99.995%). N_2 gas sorption measurements at 77 K were carried out up to 1 atm using a Micromeritics ASAP2020 instrument. Water vapor isotherms at 298 K were obtained using a Micrometrics ASAP2020 instrument equipped with a vapor source. Gas adsorption measurements of H_2 at 77 K and O_2 at 195 K were carried out up to 1 atm using a BEL Belsorp mini II instrument.

Impedance Analyses. All pellets for measuring AC impedance data were prepared by homogenously grinding the powder samples with a mortar and pestle and pressing at 1,700–4,000 kg for minutes. The thickness of the pellets ranged from 0.05 to 0.17 cm with an average diameter of 0.5 cm. For sample measurements, the pellet was placed in a homemade sample holder composed of Pt-based electrodes, which was located in an ESPEC SH-222/Benchtop temperature- and humidity-controlled chamber. For the D_2O-soaked sample, the pelletized sample was placed in a small homemade chamber into which a D_2O vapor stream was continuously flowed using a carrier gas (99.999% N_2). To equilibrate the temperature and humidity, the sample was kept in the chamber for 6–48 h before AC measurements. Further, to improve accuracy, the impedance data were collected repeatedly until value convergence was achieved. The AC measurements were carried out using a Solartron SI 1260 impedance/gain-phase analyzer and dielectric interface with Pt-pressed electrodes by applying an AC voltage amplitude of 100 mV in the frequency range of 3 MHz to 0.1 Hz. ZView and ZPlot software were used to analyze and fit the impedance plots to acquire the resistance value through a designed equivalent circuit. In particular, to correct the inductance error generated from wires, etc. in the high-frequency range, we redesigned the equivalent circuit to contain a series inductance and accurately measured the resistance from the spectra for the sulfonated sample. Then, accurate conduction values and activation energies were calculated using the equations below.

$$\sigma = \frac{L(cm)}{A(\pi r^2) * R(\Omega)} \qquad \ln(\sigma \mathrm{T}) = \ln(\sigma_o \mathrm{T}) - \frac{E_a}{K_b}(\frac{1}{\mathrm{T}})$$

Solid state NMR Study. Spin–lattice relaxation time (T_1), spin–spin relaxation time (T_2), effective transverse relaxation time (T_2*), and self-diffusion coefficient (D_s) were calculated using the following equations.

T_1 from the intensity fitting equation: $I[t] = I[0]+P\exp(-t/T_1)$

T_2 from the area fitting equation: $I[t]= P\exp(-t/T_2)$

T_2* from the solid-state ^{2}H NMR line shape, which can be fitted by a Lorentzian with a center frequency of ω and a line width of $\Delta\nu = 1/\pi T_2^*$.[1] When the exchange rate is $\Omega = 1/2\ \tau_c$,

$$\frac{1}{\Omega} = \frac{1}{\pi T_2^*}$$

$$\Omega = \Omega_0 \exp\left(-\frac{E_A}{RT}\right).$$

The self-diffusion coefficient (D_s) and its activation energy can be calculated from the following equation.[2]

$$D_s = D_0\exp(-E_a/kT)$$

Single PEMFC Test. MEAs were prepared by forming catalyst-coated gas diffusion layers. Membranes were made directly from pelletized POPs, and the thickness of the pellet was about 500 µm. Electrodes were prepared by spraying Pt/C (46.5 wt%) catalyst ink containing Nafion ionomer onto porous carbon paper (GDL, 39BC-SGL). The catalyst loading amounts were 0.2 mg cm^{-2} for the anode and 0.4 mg cm^{-2} for the cathode. The pellet was placed between two catalyst-coated electrodes using a Teflon gasket. The active areas used in the experiments were 1 and 5 cm^2. The MEA was arranged between graphite bipolar plates to obtain a single cell. The performance of the prepared single cells was assessed at 80 °C and 100% RH for both the anode and the cathode with a gas flow rate of 200 cc min^{-1} H_2 at the anode and 600 cc min^{-1} O_2 at the cathode.

Table S1. Elemental anylsis data of **1E** and **1ES**.

	1E		**1ES**	
	Calc.	Expt.	Calc.	Expt.
C	68.45	68.21	44.36	44.75
H	4.45	4.07	4.14	3.90
S	0	0	10.71	10.31
Formula	$[C_{11}H_7O_2]\cdot0.672H_2O\cdot0.294HCl$		$[C_{11}H_{6.005}O\cdot S_{0.995}O_{2.985}H_{0.995}]\cdot2.61H_2O$	

From the elemental analysis, 0.001 of aldehyde groups with respect to biphenyldicarboxaldehyde remained unreacted (Table S1 and the schematic diagram below). Sulfur was present only in **1ES**, indicating the successful sulfonation of this framework. The number of sulfonic acid based on the repeating unit indicated in the box below was estimated to be 0.995.

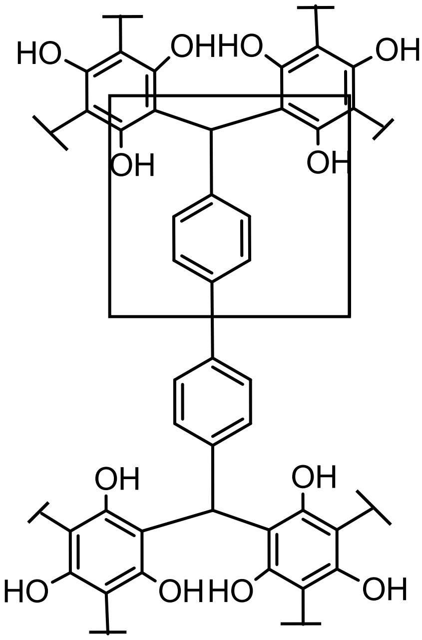

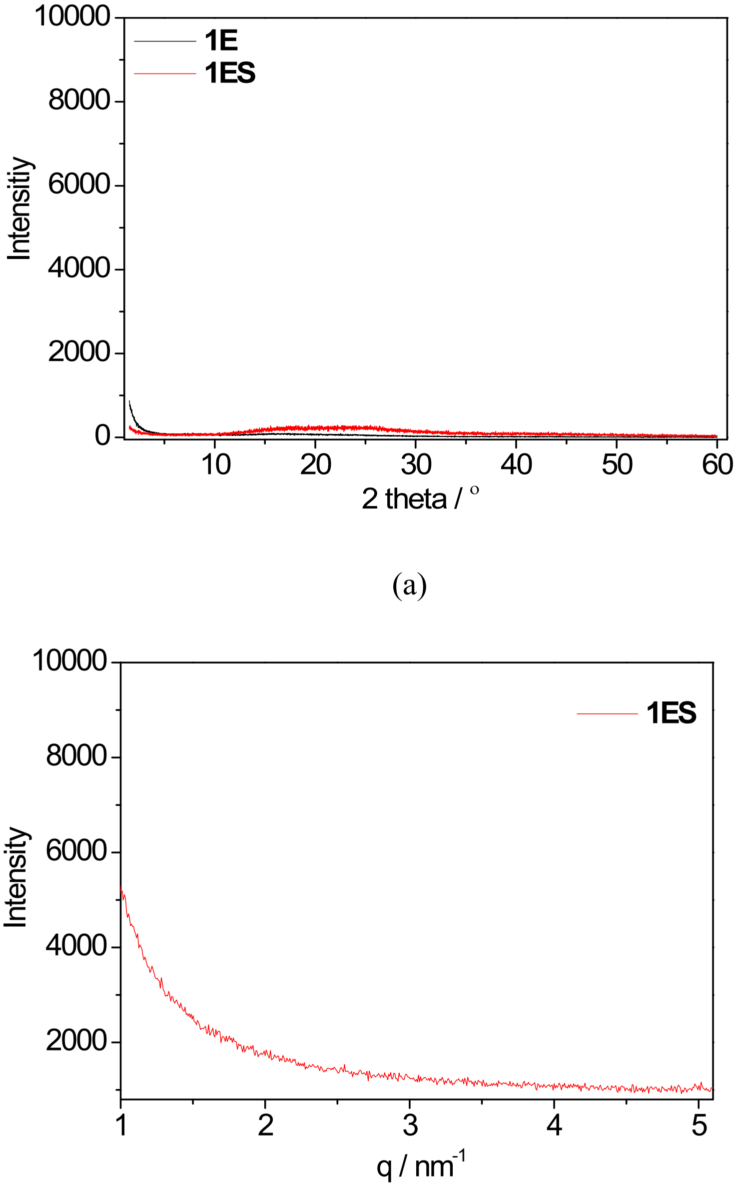

(a)

(b)

Fig. S1. (a) Powder X-ray diffraction patterns **1E** and **1ES**. (b) Small angle X-ray scattering pattern of **1ES** ($q = (4\pi/\lambda)\sin\Theta$).

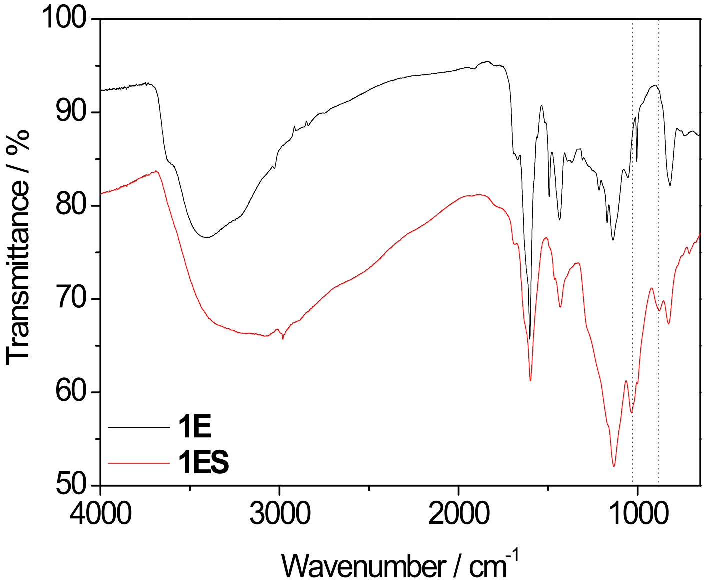

Fig. S2. IR spectra of **1E** and **1ES**.

Table S2. Peak assignments of **1E** and **1ES** in Figure S3.

ppm (number)	Assignment
193 (1)	unreacted aldehyde carbon
153 (2)	phenoxy carbon
127, 138 (3)	aromatic carbons
108 (4)	reacted phloroglucinol ortho-carbons
97 (5)	unreacted phloroglucinol ortho-carbons
68 (6)	THF residues trapped in the pores
35 (7)	tertiary carbon formed by the condensation reaction
136 (8)	sulfonated carbon in benzene

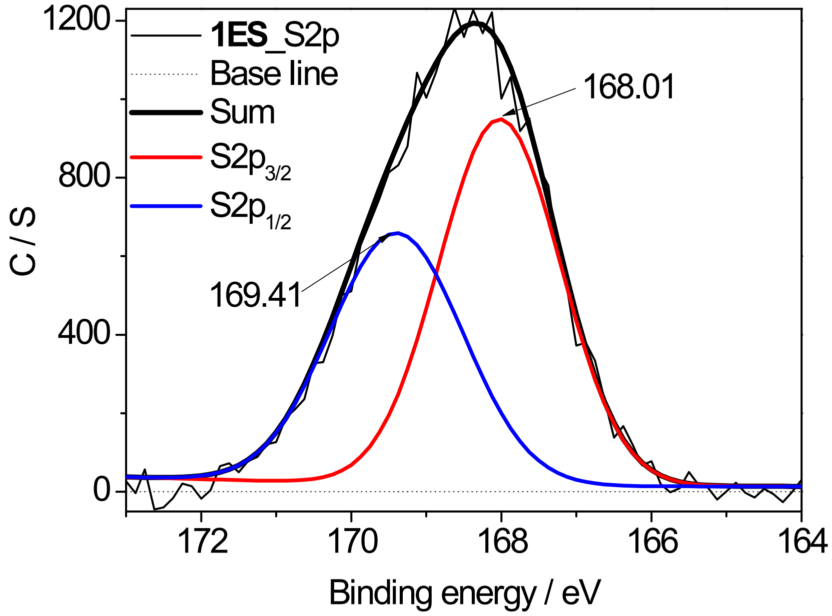

Fig. S3. Narrow scans of S2p for **1ES**.

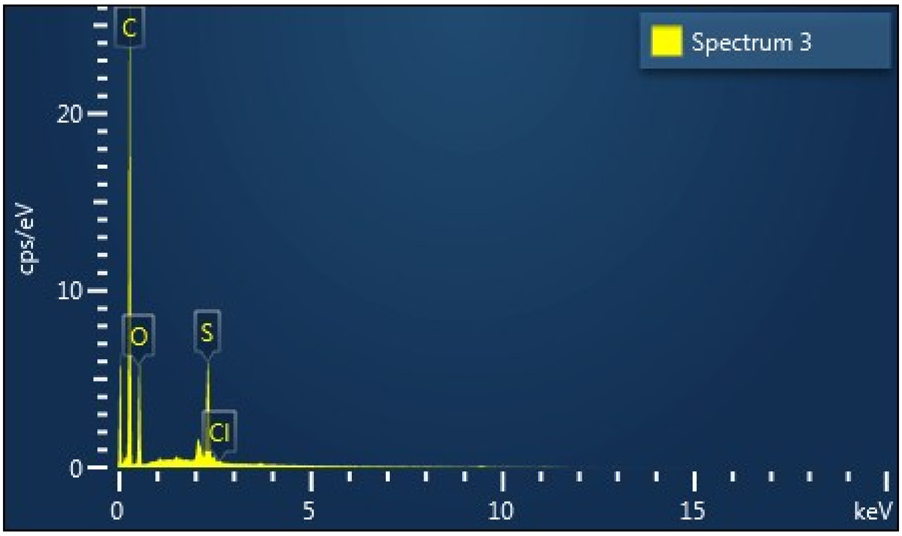

Fig. S4. EDS data for **1ES**.

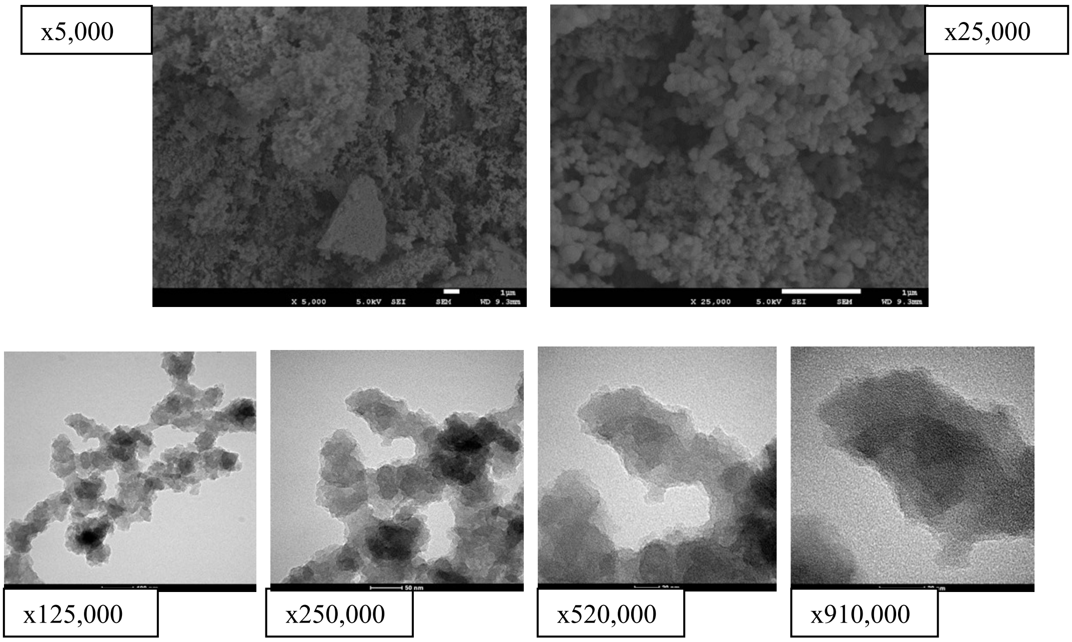

Fig. S5. SEM (top) and TEM (bottom) images of **1E**.

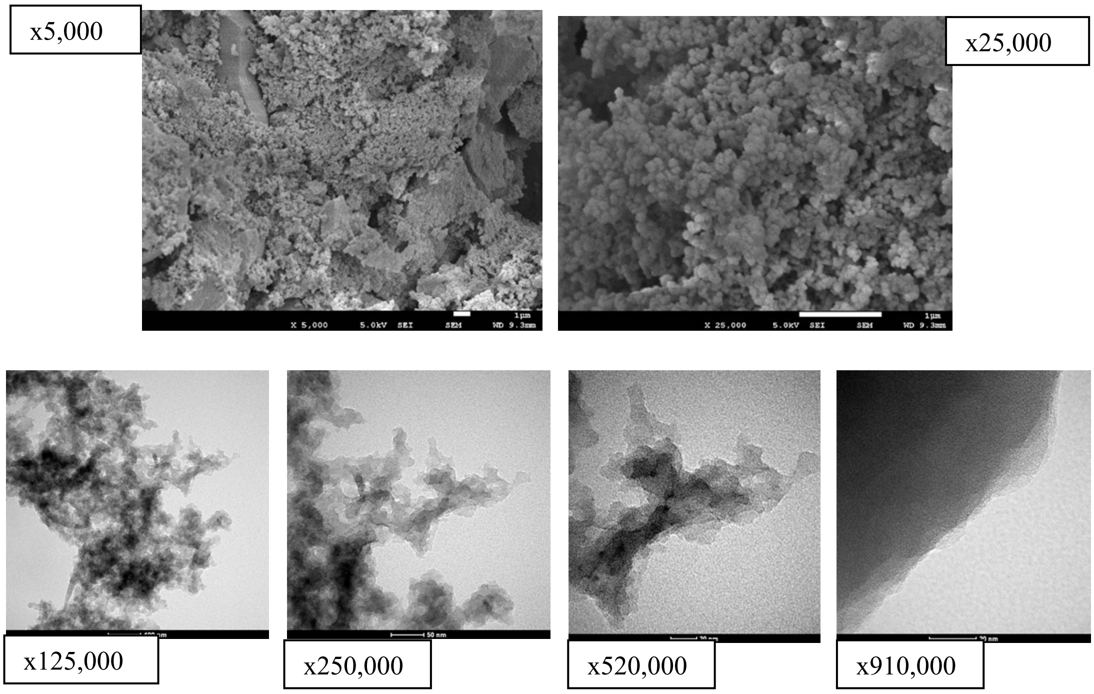

Fig. S6. SEM (top) and TEM (bottom) images of **1ES**.

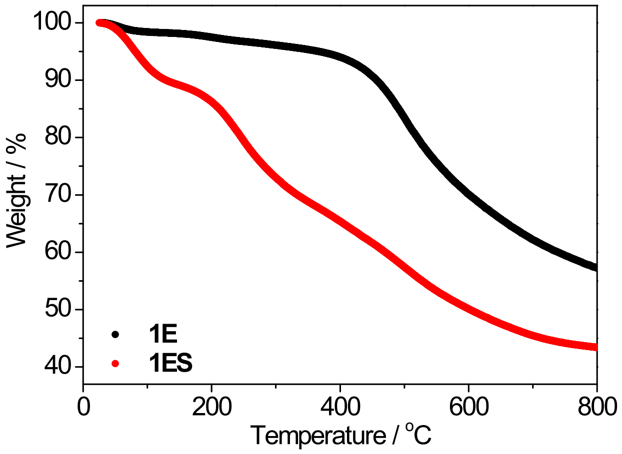

(a)

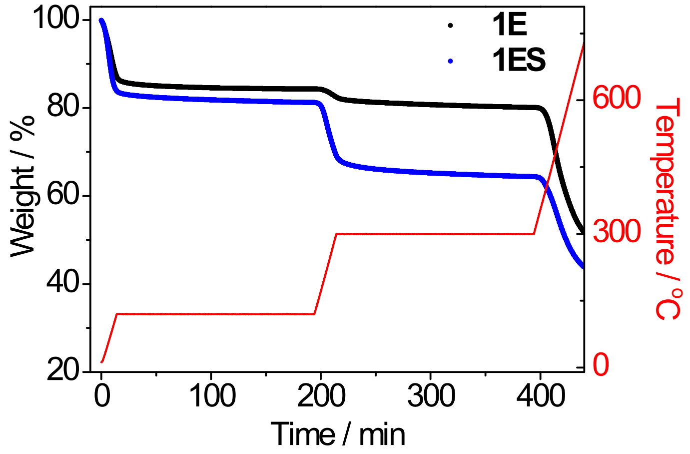

(b)

Fig. S7. (a) TGA data for **1E** and **1ES** from 25 °C to 800 °C under N_2 (99.999%) atmosphere. (b) TGA diagram for **1E** (black line) and 1**ES** (blue line) as a function of time.

The thermal stability of **1E** was superior to that of **1ES**. The initial loss (30 ~ 120 °C) in Fig. S7a was ascribed to the evaporation of solvents in the pores. After the initial loss, the stability of **1E** was maintained up to 400 °C with a slight decomposition. However, **1ES** was decomposed from 89.31 wt% to 65.37 wt% in the temperature range of 120 - 400 °C. The weight loss in this temperature range corresponded to the decomposition of sulfonic acid groups. Therefore, the thermal stability of **1E** was greater than that of **1ES** with sulfonic acid groups. To assist further understanding, thermal decompositions of the samples were measured as a function of time (Fig. 7b). To obtain distinct decomposition section, the temperature was maintained at 120 and 300 °C for 3 h. While no appreciable weight loss was observed during the retention time, the weight variation (from 84.43 to 81.94 wt%) of **1E** was small as the temperature increased from 120 to 300 °C. In contrast, in the same temperature range, there was significant weight loss (from 81.16 to 67.42 wt%) in **1ES**. After the decomposition of **1ES** at 300 °C for 3 h, elemental analysis showed that sulfur was almost absent in the sample (S: 0.59 %), which indicates the degradation of sulfonic acid groups.

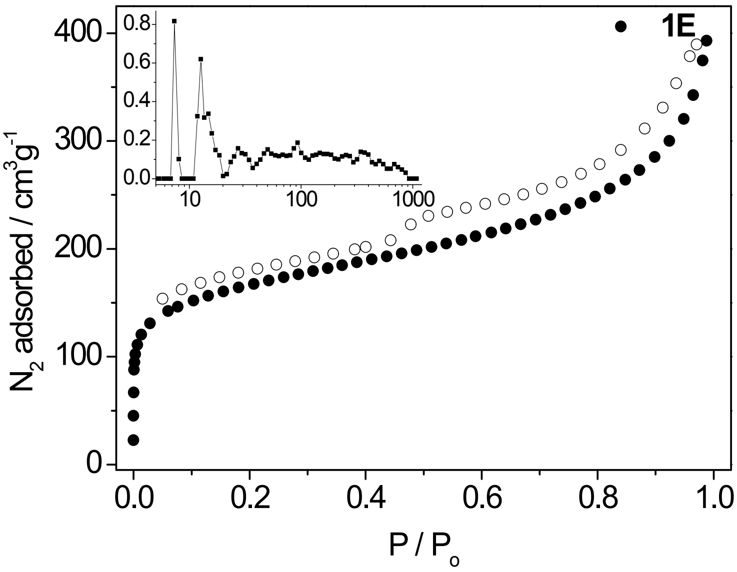

(a)

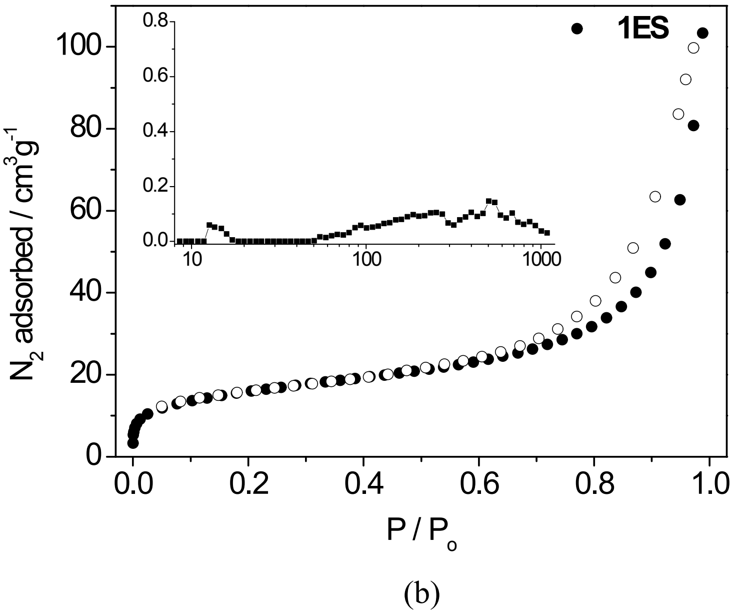

(b)

Fig. S8. N$_2$ isotherms (main panel) and DFT pore size distributions (inset) of **1E** (a) and **1ES** (b) at 77 K. Filled and open symbols indicate adsorption and desorption, respectively.

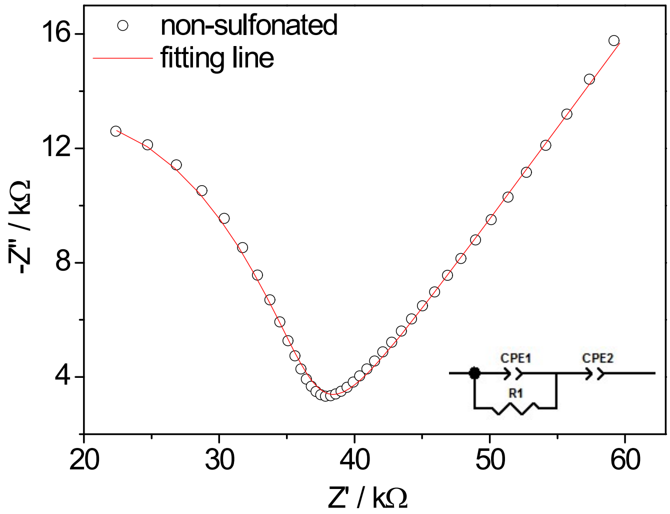

(a)

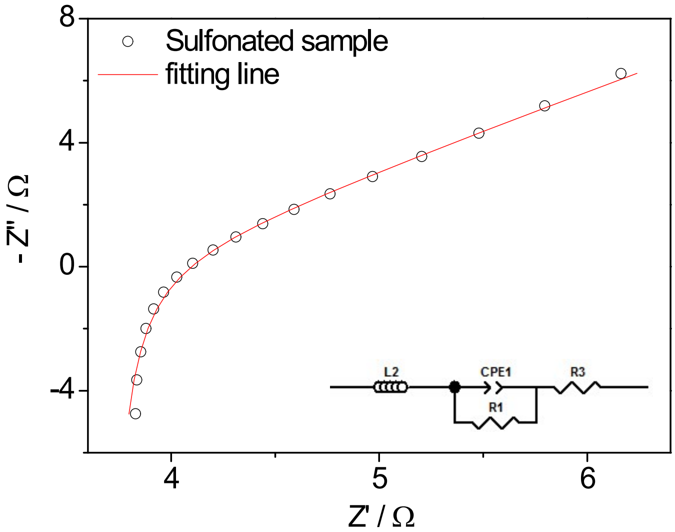

(b)

Fig. S9. Fitting line and equivalent circuit for non-sulfonated (a) and sulfonated samples (b).

Table S3. List of proton-conductive porouos organic materials and Nafion. Conductivity values and activation energies are shown under indicated conditions.

Compounds	**σ (S cm^{-1})**	**E_a(eV)**	**T(°C)**	**RH(%)**
1ES$^{\text{this work}}$	**1.59 x 10^{-1}**	**0.13**	**80**	**90**
Nafion®117[3]	1.5 x 10^{-1}		80	98
1S[4]	7.72 x 10^{-2}	0.34	80	90
Nafion[5]	5 x 10^{-2}	0.22	30	98
HOF-GS-11[6]	1.8 x 10^{-2}	0.14	30	95
HOF-GS-10[6]	7.5 x 10^{-3}	0.49	30	95
EB-COF:PW_{12}[7]	3.32 x 10^{-3}	0.24	25	97
PA@TpBpy-MC[8]	2.50 x 10^{-3}	0.11	120	0
PA@TpBpy-ST[8]	1.98 x 10^{-3}	0.12	120	0
trz@TPB-DMTPCOF[9]	1.1 x 10^{-3}	NA	130	0
PA@Tp-Azo[10]	9.9 x 10^{-4}	0.11	25	98
phytic@TpPa-(SO3H-Py)[11]	5 x 10^{-4}	0.16	120	0
phytic@TpPa-Py[11]	3.0 × 10^{-4}	0.10	120	0
1[4]	2.10 x 10^{-4}	0.35	70	90
phytic@TpPa-SO3H[11]	7.5 x 10^{-5}	NA	120	0
PA@Tp-Azo[10]	6.7 x 10^{-5}	NA	67	0
1E$^{\text{this work}}$	**1.88 x 10^{-5}**	**0.24**	**80**	**90**
TpPa-SO3H[11]	1.7 x 10^{-5}	NA	120	0
1'[4]	1.63 x 10^{-5}	0.32	70	80

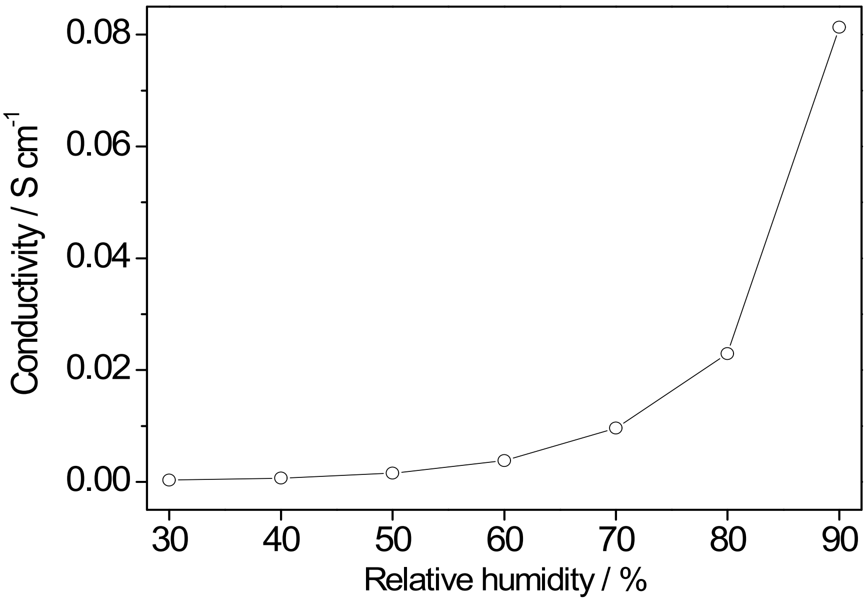

Fig. S10. Relative humidity-dependent proton conductivity for **1ES** at 25 °C.

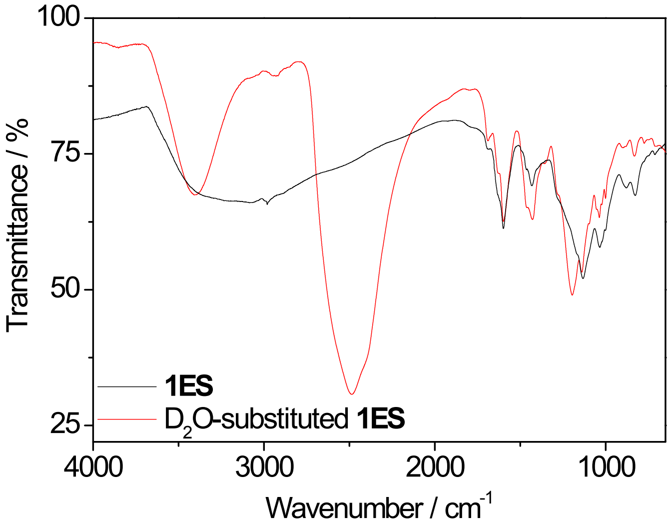

Fig. S11. IR spectrums of **1ES** and D_2O-substituted **1ES**.

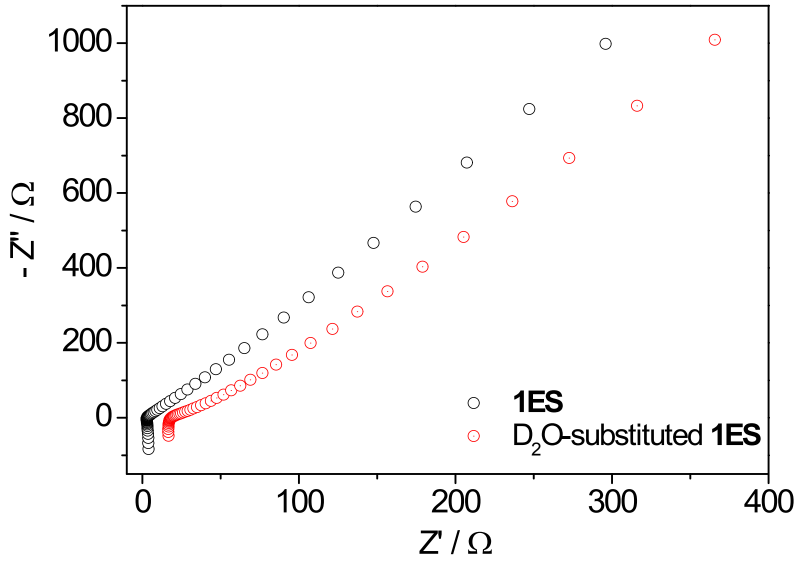

Fig. S12. Nyquist plots of **1ES** and D_2O-substituted **1ES** at 50 °C and 98% RH.

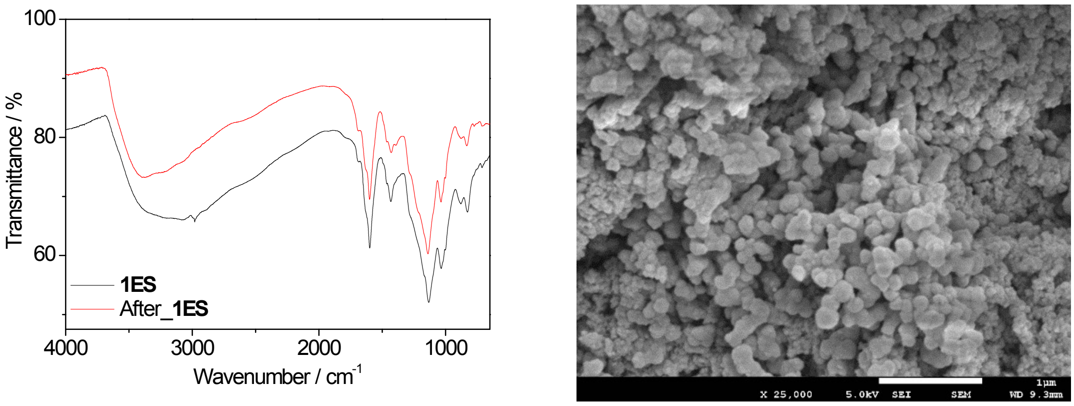

Fig. S13. IR patterns (left) and SEM image (right) of **1ES** after impedance measurements.

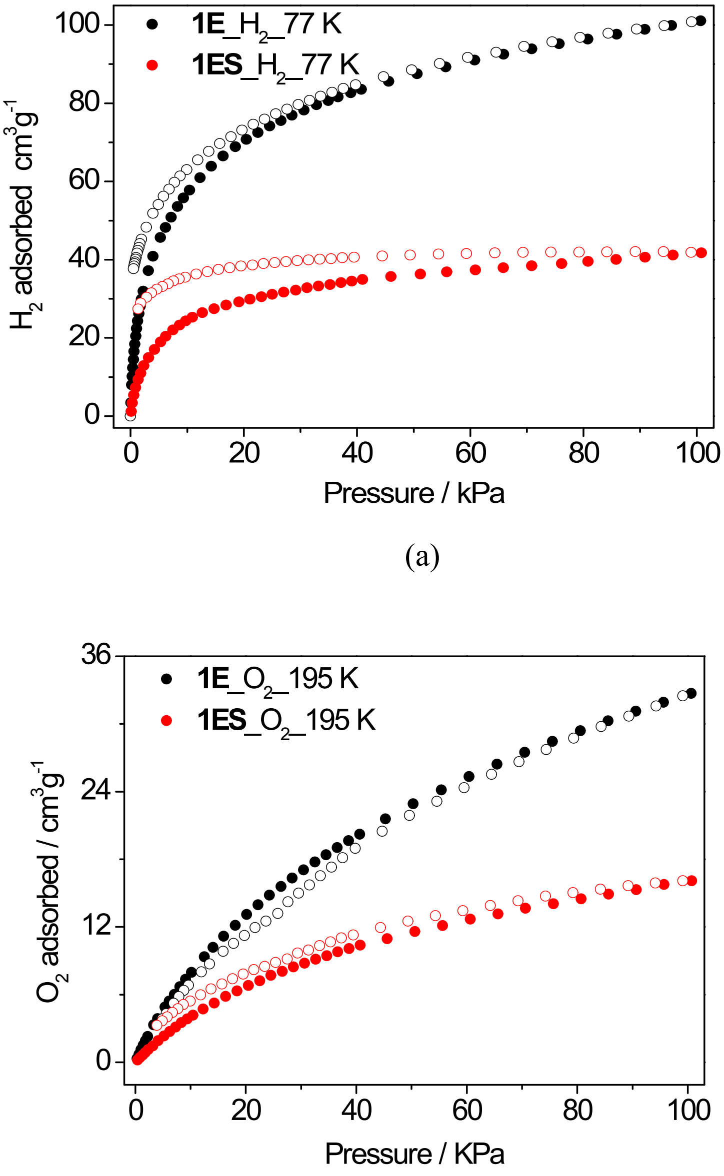

(a)

(b)

Fig. S14. (a) H_2 adsorption isotherms at 77 K and (b) O_2 isotherms at 195 K for **1E** and **1ES**.

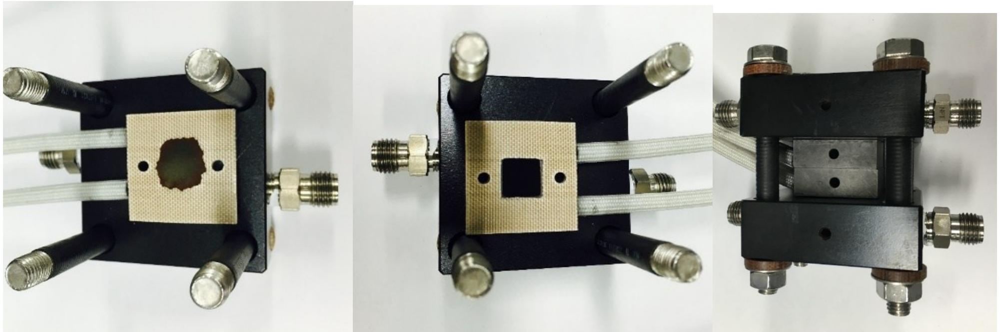

Fig. S15. Representation of membrane electrode assembly (MEA) cell: (left) gasket and catalyst-coated gas diffusion layer, (middle) gasket, catalyst-coated gas diffusion layer, and pellet, and (right) single cell.

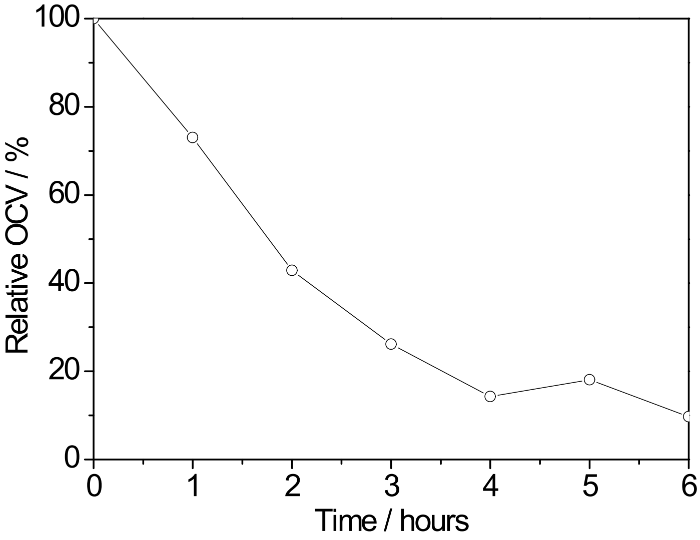

Fig. S16. The stability test of OCV for the cell using **1ES**.

[Reference]

1. Y. J. Lee, B. Bingol, T. Murakhtina, D. Sebastiani, W. H. Meyer, G. Wegner and H. W. Spiess, *J. Phys. Chem. B*, 2007, **111**, 9711–9721.
2. S. Kostinski, R. Pandey, S. Gowtham, U. Pernisz and A. Kostinski, *IEEE Electron Device Lett.*, 2012, **33**, 863-865.
3. T. Suda, K. Yamazaki and H. Kawakami, *J. Power Sources*, 2010, **195**, 4641-4646.
4. D. W. Kang, K. S. Lim, K. J. Lee, J. H. Lee, W. R. Lee, J. H. Song, K. H. Yeom, J. Y. Kim and C. S. Hong, *Angew. Chem. Int. Ed.*, 2016, **55**, 16123-16126.
5. R.C.T Slade, A Hardwick and P. G. Dickens, *Solid State Ionics*, 1983, **9**, 1093-1098.
6. A. Karmakar, R. Illathvalappil, B. Anothumakkool, A. Sen, P. Samanta, A. V. Desai, S. Kurungot and S. K. Ghosh, *Angew. Chem. Int. Ed.*, 2016, **55**, 10667-10671.
7. H. Ma, B. Liu, B. Li, L. Zhang, Y. G. Li, H. Q. Tan, H. Y. Zang and G. Zhu, *J. Am. Chem. Soc.*, 2016, **138**, 5897-5903.
8. D. B. Shinde, H. B. Aiyappa, M. Bhadra, B. P. Biswal, P. Wadge, S. Kandambethc, B. Garai, T. Kundu, S. Kurungot and R. Banerjee, *J. Mater. Chem. A*, 2016, **4**, 2682-2690.
9. H. Xu, S. Tao and D. Jiang, *Nat. Mater.*, 2016, **15**, 722-726.
10. S. Chandra, T. Kundu, S. Kandambeth, R. Babarao, Y. Marathe, S. M. Kunjir and R. Banerjee, *J. Am. Chem. Soc.*, 2014, **136**, 6570-6573.
11. S. Chandra, T. Kundu, K. Dey, M. Addicoat, T. Heine and R. Banerjee, *Chem. Mater.*, 2016, **28**, 1489-1494.